Phosphocreatine immobilization of the surface of silica and magnetite nanoparticles for targeted drug delivery*

D. V. Korolev,[a,b]★ N. V. Evreinova,[a,c] E. V. Zakharova,[d] K. G. Gareev,[d] E. B. Naumysheva,[a,e] D. V. Postnov,[e] V. N. Postnov,[a,e] and M. M. Galagudza[a,b]

[a]*Almazov National Medical Research Centre, 2 ul. Akkuratova, 197341 St. Petersburg, Russian Federation. E-mail: Korolev_DV@almazovcentre.ru*
[b]*First Pavlov State Medical University of St. Petersburg, 6—8 ul. L'va Tolstogo, 197022 St. Petersburg, Russian Federation. E-mail: galagoudza@mail.ru*
[c]*St. Petersburg State Technological Institute (Technical University), 26 Moskovsky prosp., 190013 St. Petersburg, Russian Federation. E-mail: zna47@lti-gti.ru*
[d]*St. Petersburg Electrotechnical University "LETI", 5 ul. Prof. Popova, 197376 St. Petersburg, Russian Federation. E-mail: kggareev@yandex.ru*
[e]*St. Petersburg State University, 7/9 Universitetskaya nab., 199034 St. Petersburg, Russian Federation. E-mail: postnovvn@mail.ru*

A method is proposed for immobilization of anti-ischemic drug phosphocreatine on the surface of aminated silica and magnetite nanoparticles of similar size and shape. The synthesis of spacer and the coordination-ionic drug immobilization technique are described. Magnetite nanoparticles demonstrated much more efficient chemisorption of phosphocreatine than silica nanoparticles. The method was recommended for practical application.

Key words: magnetite nanoparticles, silica nanoparticles, amination, phosphocreatine, immobilization.

Targeted drug delivery enables selective accumulation of a drug within the tissue affected by a pathological process and reduction of systemic toxicity symptoms.[1] The effect is achieved by binding drug molecules to a nanoparticulate carrier followed by parenteral administration of suspensions obtained. At present, various nanocarriers are available.[2] Depending on the chemical structure of both components of a drug delivery system, reversible binding of the drug to the carrier can be realized using different strategies from physisorption to covalent bonding and nanoencapsulation. Accumulation of drug-loaded nanoparticles in the damaged tissue is due to either increased vascular permeability or specific interaction of ligands grafted to the nanoparticle surface with molecular damage markers on the plasma membrane. Silica-based materials are widely used in this field.[3] Recent research into active targeted drug delivery involves the development of methods for manipulation of drug-loaded magnetic nanoparticles in the damaged tissue using external or internal magnetic field.[4,5]

The aim of this work was to develop methods for immobilization of anti-ischemic drug phosphocreatine manufactured under the name Neoton (see Ref. 6) on the surface of silica and magnetite nanoparticles (NPs) of similar size and shape and to compare the efficiency of drug binding to them.

Experimental

We used (i) Polysorb 300 silica NPs[7] preliminarily modified following a known procedure[8] and (ii) magnetite NPs synthesized following a published procedure[9] and modified with (3-aminopropyl)triethoxysilane (APTES) in benzene.

Digital images of NPs were obtained using a JEOL JEM-1400 transmission electron microscope (Japan) with field-emission cathode, equipped with a STEM digital imaging/scanning circuitry.

* Based on the materials of the IV Interdisciplinary Symposium on Medicinal, Organic, Biological Chemistry and Pharmaceutics (MOBI-ChemFarma 2018) (September 23—26, 2018, Novyi Svet, Crimea).

Published in Russian in *Izvestiya Akademii Nauk. Seriya Khimicheskaya,* No. 5, pp. 1096—1101, May, 2019.
1066-5285/19/6805-1096

The remagnetization curves were recorded using a Lake Shore 7410 vibrating sample magnetometer (Lake Shore Cryotronics Inc., USA) in air at ambient temperature.

Surface immobilization of the drug involved preliminary amination of NPs using gas-phase and liquid-phase techniques. The former was applied to silica NPs since they initially existed as dry powder and it was possible to carry out the synthesis in the pseudo-boiling gas-phase regime. Magnetite NPs were prepared as suspensions, so it was more appropriate to carry out liquid-phase amination in organic medium. In both cases the aminating agent was APTES (Scheme 1).

Scheme 1

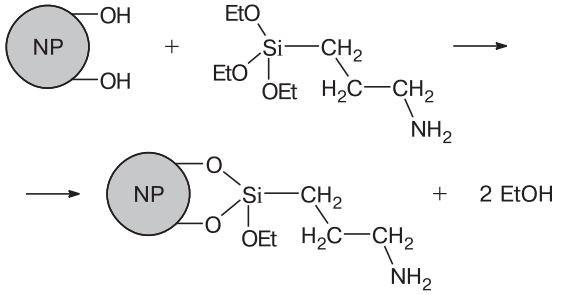

Surface modification of silica NPs. To carry out gas-phase modification of silica NPs with amino groups a procedure involving chemsorption of APTES from the gas phase in a flow reactor was developed. The design of the reactor provided evaporation of the reagent at 220 °C, chemisorption, and removal of the excess reagent and side products of the reaction. The carrier gas was nitrogen. The method involved removal of bound water from the NP surface at 250 °C for 2 h, chemisorption of APTES at 250 °C for 1 h, and subsequent removal of the excess amounts of reagents and side products at the same temperature over a period of 2 h.[8]

Surface modification of magnetite NPs. A suspension of magnetite NPs was freeze-dried on a Vaco 2 freeze dryer (ZirBus, Germany) at −50 °C and a pressure of 3 Pa. A 50-mL round-bottom flask was charged with dry magnetite NPs (2 g) and 25 mL of 5% APTES solution in dried benzene. The reaction medium was refluxed for 2 h at 80 °C using a thermostatted cell connected to a LT-105a thermostatic bath circulator (LOIP Ltd., Russia). The excess reagent was removed by multiply washing with anhydrous chloroform using magnetic separation and ethanol (at the final stage). During the modification and washing the reaction mixture was vigorously stirred with a magnetic stir bar.

Determination of the content of amino groups in the samples. To aminated magnetite NPs, 0.1 N hydrochloric acid (1 mL) was added and the mixture was periodically shaken over a period of 15 min to neutralize amino groups. Then, the suspension was centrifuged at 3000 rpm for 5 min. The supernatant liquid was titrated with 0.1 N solution NaOH with methyl orange as pH indicator. The eventual total amount of amino groups was calculated from the amount of alkali.

It is impossible to evaluate the amount of drug that can be chemisorbed on the modified surface from the total amount of amino groups. The content of accessible amino groups was determined using indocyanine green (ICG) fluorescent dye. Immobilization is schematically shown in Fig. 1, *a*. To a suspension containing preliminarily aminated NPs (50 mg) in water (2 mL), a solution of ICG (1 mL, 1 mg mL^{-1}) and distilled water (1 mL) was added. The sorption experiments were carried out in 15-mL polypropylene tubes using an LS-220 shaker (LOIP Ltd., Russia) over a period of 2 h at a stirring rate of 300 rpm. Then the solution was centrifuged at 3000 rpm for 5 min and washed five times with distilled water and then centrifuged again.

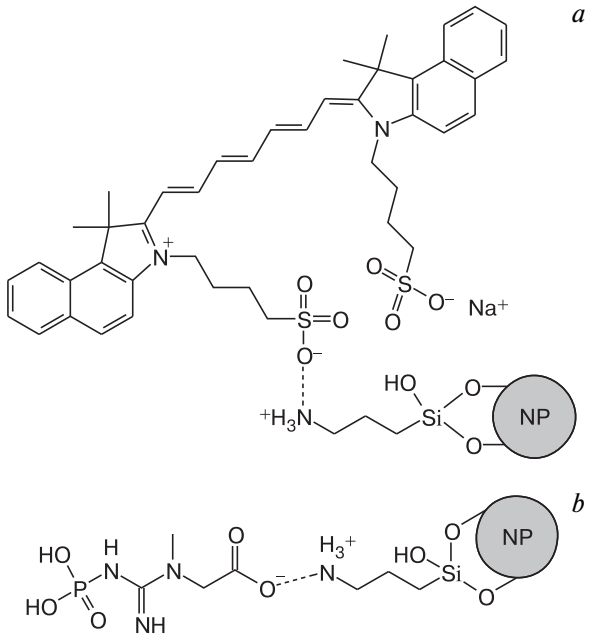

Fig. 1. Immobilization of fluorescent dye ICG (*a*) and phosphocreatine (*b*).

Having completed the ICG sorption experiments, the amount of the dye sorbed was determined. To this end, 0.1 N NaOH (10 mL) was added to the residue and a 15-min desorption experiment was carried out. Then, the mixture was centrifuged and the supernatant liquid (1 mL) was sampled. The ICG content was determined spectrophotometrically by analyzing the solution thus obtained using an Unico 2802S instrument (Unico Sys, USA) at a wavelength (λ) of 700 nm.

Phosphocreatine immobilization on NP surface. To aminated NPs (50 mg), 0.1 N aqueous NaOH (1 mL) and 1 mL of a solution of phosphocreatine in 0.1 N HCl (2 mg mL^{-1}) was added. The sorption experiments were carried out in 15-mL polypropylene tubes over a period of 2 h using an LS-220 shaker (LOIP Ltd., Russia) at a stirring rate of 300 rpm. Then the solution was centrifuged at 3000 rpm for 5 min and washed five times with distilled water and then centrifuged again. Immobilization of phosphocreatine on the NP surface is schematically shown in Fig. 1, *b*.

The qualitative composition of the freeze-dried samples was studied using a Nicolet 8700 IR Fourier spectrometer (Thermo Scientific, USA) and bulk samples using an integrating sphere. Spectral measurements were carried out in the range of 4000—400 cm^{-1}.

The method for determination of phosphocreatine levels was developed taking into account the fact that in aqueous alkali solution this compound undergoes a ready transformation into

creatinine upon elimination of phosphoric acid (Scheme 2). This transformation can be detected with ease using the Jaffe reaction[10] that is based on the reaction of creatinine with sodium picrate.

Scheme 2

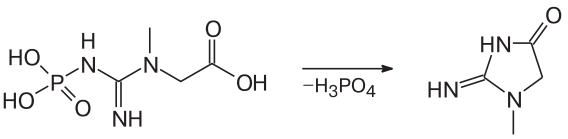

Creatinine reacts with alkaline picrate to give a red complex. A change in the optical density of the newly formed complex at $\lambda = 510$ nm is proportional to the concentration of creatinine in the sample. The optical densities of the absorption spectra were determined using an Unico 2802S spectrophotometer (Unico Sys, USA).

The optical densities of the solutions containing different amounts of phosphocreatine were identical to that of the blank sample. This is indicative of the absence of the phosphocreatine → creatinine transition.

To study this fact in more detail, a solution of the blank sample of picric acid and a solution with the maximum content of phosphocreatine (21.1 μg) were prepared and then the absorption spectra of the solutions were recorded in the λ range of 450—1100 nm using the spectrophotometer. No creatinine absorption band (500—600 nm) was observed at the maximum content of phosphocreatine in the sample.

Since the determination of phosphocreatine using the Jaffe reaction failed, a known procedure[11] involving diacetyl in the presence of α-naphthol was employed to evaluate the amount of free phosphocreatine. A 1% alkali solution of α-naphthol was used. The alkali solution contained NaOH (6 g) and Na_2CO_3 (16 g) in 100 mL of water. The diacetyl solution was prepared immediately prior to measurements and adjusted to a concentration of 0.05%.

To study the applicability of the method to the determination of phosphocreatine, a blank sample and a sample with the maximum concentration of phosphocreatine were prepared. The absorption spectra of the samples were recorded with the Unico 2802S instrument in the λ range of 450—1100 nm. Figure 2 shows that the absorption spectra of the samples analyzed at 540 nm exhibit a shift of the absorption band, which depends on the drug concentration. Subsequent analysis was performed at $\lambda = 540$ nm.

To determine the concentration of phosphocreatine chemisorbed on the surface of silica NPs, 0.1 N NaOH (5 mL) was added to the sample obtained after the chemisorption experiments and then a desorption experiment was carried out for 15 min under hand shaking. The solution thus prepared was centrifuged and then the supernatant liquid (1 mL) was sampled and analyzed for free phosphocreatine as described above at $\lambda = 540$ nm.

To determine phosphocreatine in the freeze-dried samples from the phosphorus content, weighed samples were treated with nitric acid for 1 h on a water bath at 100 °C and then analyzed on an MGA-915-MD atomic absorption spectrometer (Lumex, Russia).

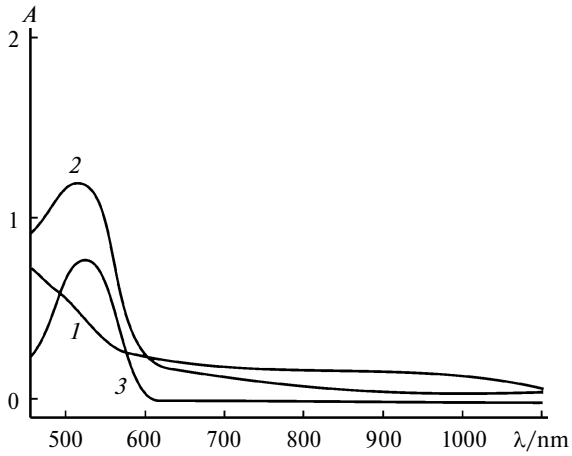

Fig. 2. Absorption spectra of blank sample (*1*) and of the sample with maximum concentration of phosphocreatine (*2*), and the sample with maximum content of phosphocreatine recorded relative to the blank sample (*3*).

Results and Discussion

The TEM images of the initial silica and magnetite NPs are presented in Fig. 3. Since the thickness of the APTES coating was not determined by electron microscopy, corresponding TEM images are not shown. Both bulk samples represent nanoparticulate powders with nearly spherical NPs. The average particle size was 8±2 nm for silica NPs and 15±5 nm for magnetite NPs.

The remagnetization curves of the samples of magnetite NPs are presented in Fig. 4. The saturation mass magnetizaton of the samples was 61 A m^2 kg^{-1} for untreated magnetite NPs and 65 A m^2 kg^{-1} for aminated magnetite NPs. This is consistent with the published data (63 A m^2 kg^{-1}) for individual similar-size magnetite nanoparticles used for magnetically controlled delivery of drugs and fluorophores.[12] Some increase in the saturation mass magnetizaton of the sample containing aminated magnetite NPs seems to be due to partial reduction of the mixed oxide to magnetite, which is additionally followed by an increase in the average magnetite grain size. This assumption is supported by an increase in the coercive force of aminated magnetite NPs (see Fig. 4, *b*). The measured coercive force of magnetite NPs was 2.5—3.0 kA m^{-1}, which corresponds to the monodomain rather than superparamagnetic state of NPs. Taking into account the size of magnetite NPs and TEM data, this can be explained by magnetostatic interaction between certain superparamagnetic iron oxide grains present in aggregates.[13]

The IR spectra of the initial and aminated samples and of the samples containing immobilized phosphocreatine are presented in Fig. 5 for silica NPs and in Fig. 6 for magnetite NPs.

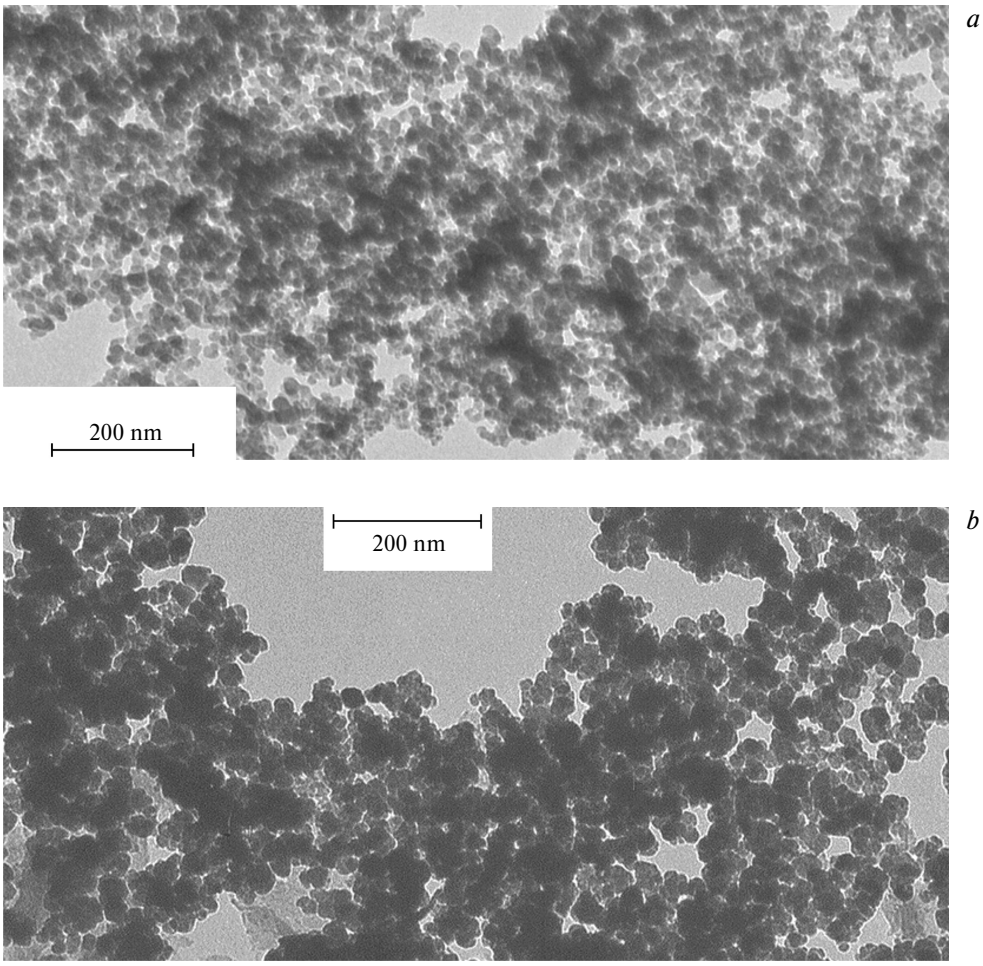

Fig. 3. TEM images of the starting nanomaterials: silica NPs (*a*) and magnetite NPs (*b*).

To analyze the evolution of the IR spectra, published data[14] were used. Since we expected a rather low content of amino groups, only medium-intensity and strong lines were analyzed. The spectra of aminated samples exhibited lines corresponding to stretching vibrations of amines in the range of 2000—3000 cm^{-1} and lines corresponding to

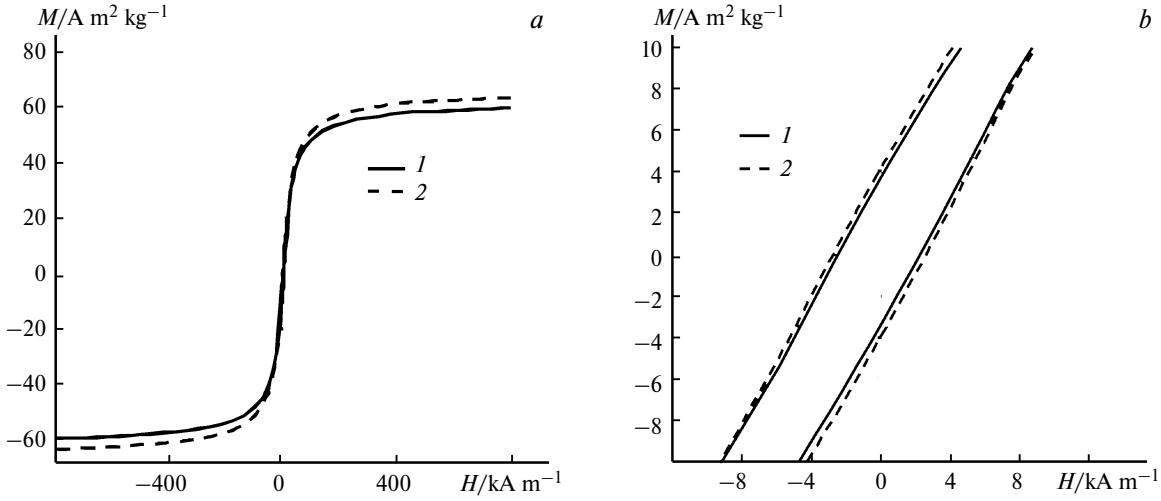

Fig. 4. Remagnetization curves of untreated (*1*) and aminated (*2*) samples of magnetite NPs: general view (*a*) and low-field region (*b*).

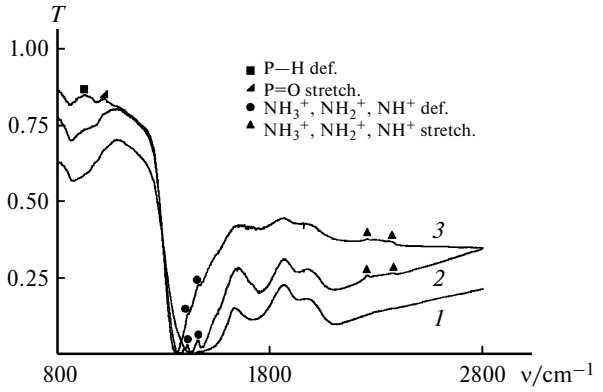

Fig. 5. IR spectra of samples based on silica NPs: untreated (*1*), aminated (*2*), and containing immobilized phosphocreatine (*3*).

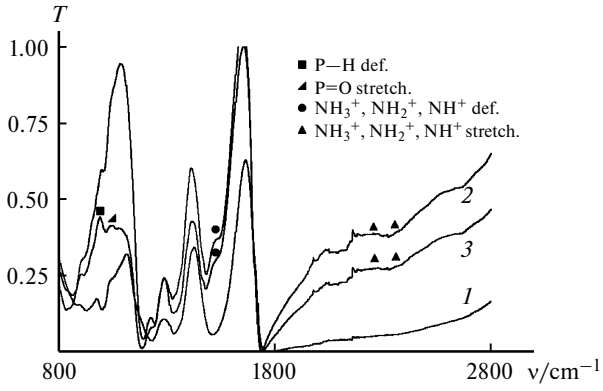

Fig. 6. IR spectra of samples based on magnetite NPs: untreated (*1*), aminated (*2*), and containing immobilized phosphocreatine (*3*).

deformation vibrations at 1460—1600 cm^{-1}, the latter being much weaker in the spectra of magnetite NPs. Probably, they overlap with the lines corresponding to water in different states. The IR spectra of the aminated silica and magnetite NPs also exhibit lines corresponding to amines. We also identified lines of P—H deformation vibrations (910—1090 cm^{-1}) and P=O stretching vibrations (960–1300 cm^{-1}); this is indicative of the presence of phosphate group which can be associated with phosphocreatine.

The results of determination of the total amount and content of accessible amino groups are listed in Table 1.

Table 1. Total amount of amino groups and the content of accessible amino groups in samples

Sample	Total amount of amino groups	Content of accessible amino groups
	mmol g^{-1}	
Silica NPs	0.20	0.0130
Magnetite NPs	0.81	0.0480

The content of accessible amino groups is about an order of magnitude lower than the total amount of amino groups in the sample. This situation is quite typical and has been reported elsewhere.[1,5]

The content of phosphocreatine on the surface of silica NPs determined spectrophotometrically by the method involving the addition of diacetyl in the presence of α-naphthol was 0.04 mg, which corresponds to a concentration of 0.8 mg or 0.0038 mmol per 1 g of carrier. We failed to determine the amount of the drug on the surface of magnetite NPs using this technique since magnetite is alkali soluble, which precludes the determination in the spectral range of the method used.

The results of the determination of phosphocreatine content by atomic absorption spectroscopy (AAS) are listed in Table 2.

The amount of phosphocreatine in the samples based on silica NPs determined by AAS is equal to that determined spectrophotometrically. The content of phosphocreatine immobilized on the surface of aminated magnetite NPs is tenfold higher than that found in the samples containing silica NPs. This is most probably due to two factors. First, liquid-phase amination involves the formation of a thicker APTES polymeric shell containing numerous amino groups. This is confirmed by the results of analysis for amino groups (see Table 1). Second, the surface of magnetite NPs is more hydroxylated, which also facilitates a complete amination. Based on the results of AAS analysis of the degree of usage of amino groups, it was found that the mole fraction of phosphocreatine bound to accessible amino groups was about 80%.

The immobilization strategy developed in this work is based on the assumption that chemisorption of carboxyl-containing organic compounds on aminated nanoparticles is possible.[1] The model carboxyl-containing drug with pronounced anti-ischemic activity was phosphocreatine which improves metabolism in myocardium and skeletal muscles. The chemical structure of phosphocreatine is identical to that of endogenous macroergic compound phosphocreatine. Phosphocreatine retards the disruption of sarcolemma in ischemic cardiomyocytes and provides intracellular energy transport. The drug improves microcirculation and thus decreases the area of ischemic necrosis. It also produces an antiarrhythmic effect in ischemia and post-ischemic reperfusion due to a decrease in ven-

Table 2. Determination of the content of phosphocreatine by atomic absorption spectroscopy

Sample	Phosphocreatine content	
	mmol g^{-1}	mg g^{-1}
Silica NPs	0.0038	0.8
Magnetite NPs	0.0380	8.0

tricular ectopic activity and maintenance of the physiological function of Purkinje fibers. Our study showed that phosphocreatine can be chemisorbed on the surface of both silica and magnetite NPs. The latter demonstrated a much more efficient immobilization of phosphocreatine. This allows one to hope for future practical application of magnetically controlled anti-ischemic drug delivery.

This work was carried out on facilities at the Centre for Optical and Laser Materials Research and at the Centre for Innovative Technologies of Composite Nanomaterials (both at St. Petersburg State University).

This work was financially supported by the Russian Foundation for Basic Research (Project No. 17-00-00272).

References

1. M. Galagudza, D. Korolev, D. Sonin, V. Postnov, E. Shlyakhto. *J. Manufacturing Technology Management*, 2010, **8**, 930.
2. A. F. Mironov, K. A. Zhdanova, N. A. Bragina, *Russ. Chem. Rev.*, 2018, **87**, 859.
3. O. B. Gorbatsevich, D. N. Kholodkov, T. S. Kurkin, Yu. N. Malakhova, D. R. Streltsov, A. I. Buzin, V. V. Kazakova, A. M. Muzafarov, *Russ. Chem. Bull.*, 2017, **66**, 409.
4. E. M. Kostyukhin, L. M. Kustov, *Mendeleev Commun.*, 2018, **28**, 559.
5. D. V. Korolev, M. M. Galagudza, M. V. Afonin, I. S. Uskov, V. B. Ostashev, E. A. Umenyshkina, I. V. Aleksandrov, *Biotekhnosfera* [*Biotechnosphere*], 2012, **19**, 2 (in Russian).
6. S. A. Kovalev, V. N. Belov, O. A. Osipova, *Vestn. Eksp. Klin. Khirurgii*, 2015, **29**, 314 [*J. Exper. Clinical Surgery*, 2015, **29**].
7. D. A. Markelov, O. V. Nitsak, I. I. Gerashchenko, *Pharm. Chem. J.*, 2008, **7**, 30.
8. D. V. Korolev, K. Yu. Babikova, V. N. Postnov, E. B. Naumysheva, G. V. Papayan, E. I. Pochkaeva, D. L. Sonin, *Biotekhnosfera* [*Biotechnosphere*], 2016, **47**, 42 (in Russian).
9. Y. G. Toropova, A. S. Golovkin, A. B. Malashicheva, A. N. Gorshkov, K. G. Gareev, M. V. Afonin, D. V. Korolev, M. M. Galagudza, *Int. J. Nanomed.*, 2017, **12**, 593.
10. A. Nessar, *Clinical Biochemistry*, Oxford University Press, New York, 2011, p. 72.
11. S. E. Severina, *Praktikum po biokhimii: uchebn. posobie* [*A Laboratory Course on Biochemistry*], Izd-vo MGU, Moscow, 1989, p. 189 (in Russian).
12. O. Chen, L. Riedemann, F. Etoc, H. Herrmann, M. Coppey, M. Barch, C. T. Farrar, J. Zhao, O. T. Bruns, H. Wei, P. Guo, J. Cui, R. Jensen, Y. Chen, D. K. Harris, J. M. Cordero, Z. Wang, A. Jasanoff, D. Fukumura, R. Reimer, M. Dahan, R. K. Jain, M. G. Bawendi, *Nat. Commun.*, 2014, **5**, 5093.
13. P. V. Kharitonskii, K. G. Gareev, S. A. Ionin, V. A. Ryzhov, Yu. V. Bogachev, B. D. Klimenkov, I. E. Kononova, V. A. Moshnikov, *J. Magnetics*, 2015, **20**, 221.
14. J. C. D. Brand, G. Eglinton, *Applications of Spectroscopy to Organic Chemistry*, Oldbourne Press, London, 1965, 279.

Received October 24, 2018;
in revised form March 18, 2019;
accepted March 25, 2019